

Wobbling motion in band crossing

Makito Oi ^{a,c} ¹, Naoki Onishi ^{a,c}, Takatoshi Horibata ^{b,c}

^a*Institute of Physics, Graduate School of Arts and Sciences, University of Tokyo,
Komaba, Meguro-ku, Tokyo 153-8902, Japan*

^b*Department of Information System Engineering, Aomori University, Kobata,
Aomori 030-0943, Japan*

^c*Cyclotron Laboratory, Institute of Physical and Chemical Research
(RIKEN), Hirosawa 2-1, Wako-city, Saitama 351-0198, Japan*

Abstract

To study the wobbling motion in the band crossing region GCM calculations are performed using the angular momentum projected wave functions. The method corresponds to the variation after projection, which can include a description of dynamical correlations between collective and single-particle degrees of freedom. We found a sharp band crossing between a low- K band and a high- K band in which these two states are coupled through a “wobbling state” in backbending region. We discuss a mechanism of band crossing involving both low- K and high- K states.

Key words: Wobbling, Backbending, Tilted rotation

PACS number(s): 27.70.+q, 21.10.-k

The backbending phenomenon was discovered early in 1970's [1] in pursuit of high spin physics. Several physical interpretations were proposed: triaxial deformation [2,3]; Mottelson-Valatin effect [4]; etc. With many theoretical efforts [5,6], it is established that the “rotational alignment” plays a major role in the phenomenon. The rotational alignment occurs in high- j orbitals due to the Coriolis force. The backbending phenomenon is explained in terms of band crossing of a g-band (ground state band) with an s-band (rotational aligned band). Both of the bands are considered to involve a low- K intrinsic state.

Recent papers on experiments in $A=180$ region [7–10] report observations of band crossings between the g-band and a high- K band. (for example, $K^\pi = 8^+$

¹ e-mail address: mon@nt4.c.u-tokyo.ac.jp

in ^{182}Os and ^{180}W). The backbending phenomenon accompanied with this high- K band crossing seems to be caused by another mechanism different from the usual rotational alignment. Walker et al. speculated [10] that the high- K band is characterized as a tilted rotational band (t-band) as per the following facts:

In $A \sim 180$ nuclei, the Fermi level is in the middle of the high- j orbital. Hence excited single-particle states tend to have substantial angular momentum components of both the intrinsic 1-axis (rotating axis) and 3-axis (symmetry axis of quadrupole deformation). These nuclei have dual features of the rotational alignment and the deformation alignment.

They considered the tilted rotation in the high- K band as a *uniform* rotation around a *fixed* axis tilted from the principal axes, according to the tilted axis cranking model (TAC) [11]. There remains, however, a question about explanation of nature and mechanism of the new type of backbending by using TAC because their consideration implied that the backbending was caused by a sudden directional change of rotating axis, i.e., a quick transition from principal axis cranking to tilted axis cranking, but this mechanism seems somewhat too simple for a description of a quantum many-body phenomenon, because TAC states are constructed by a single configuration having a classical picture.

We take a quantal approach for such a band crossing mechanism: the generator coordinate method (GCM) after angular momentum projection (AMP) [12,13], where a 3d-cracked HFB (3d-CHFB) state is employed as the generating function. The method corresponds to the variation after projection, which can take account of the dynamical coupling of intrinsic motion with collective rotation in a fully quantum mechanical framework. In this manner, we can deal with general rotations such as wobbling motion. Tilting angles θ, ϕ are defined in the angular momentum constraints in self-consistent 3d-CHFB calculations as,

$$\langle \hat{J}_1 \rangle = J \sin \theta \cos \phi, \quad \langle \hat{J}_2 \rangle = J \sin \theta \sin \phi \quad \text{and} \quad \langle \hat{J}_3 \rangle = J \cos \theta. \quad (1)$$

Throughout calculations presented in this letter, J is taken to be $13\hbar$ because the stable solutions rotating around a tilted axis ($|\varphi(\theta = 28^\circ, \phi = 0^\circ)\rangle$) appear in the previous 3d-CHFB calculations at this value of J and the higher [14]. Prescriptions of generating the intrinsic states are explained in detail in Ref.[14]. The tilting angles are used as generator coordinates. In this letter the

azimuthal angle ϕ is, however, fixed to be zero for the sake of simplification in numerical calculations. Thus the GCM ansatz is written as,

$$|\Phi_M^I\rangle = \sum_{K=-I}^I \int_{-\theta_0}^{\theta_0} d\theta f_K^I(\theta) \hat{P}_{MK}^I |\varphi(\theta)\rangle, \quad (2)$$

where \hat{P}_{MK}^I is the AMP operator and $|\varphi(\theta)\rangle$ represents a 3d-CHFB state. The angular momentum projection performed here is exact and three-dimensional[15]. With this ansatz, a high-spin state is expressed as a superposition of eigenstates of angular momentum with different orientations of the rotating axis and different K -quantum number. Namely, the ansatz takes *wobbling motion* into account in a quantum mechanical manner.

Variation leads to the so-called the Hill-Wheeler equations:

$$\sum_{K'} \int d\theta' \left(H_{KK'}^I(\theta, \theta') - E^I N_{KK'}^I(\theta, \theta') \right) f_{K'}^I(\theta') = 0. \quad (3)$$

The norm overlap matrix $N_{KK'}^I(\theta, \theta')$ and the energy overlap matrix $H_{KK'}^I(\theta, \theta')$ are defined,

$$N_{KK'}^I(\theta, \theta') = \langle \varphi(\theta) | \hat{P}_{KK'}^I | \varphi(\theta') \rangle, \quad (4)$$

and

$$H_{KK'}^I(\theta, \theta') = \langle \varphi(\theta) | \hat{H} \hat{P}_{KK'}^I | \varphi(\theta') \rangle, \quad (5)$$

respectively.

We solve Eq.3 in two steps [16]: 1) Diagonalize the norm overlap matrix $N_{KK'}^I(\theta, \theta')$ with respect to both magnetic quantum number (K) and tilting angle (θ) to obtain eigenvalues ν_n^I and eigenfunctions $\chi_n^I(\theta; K)$ (n is an index specifying the n -th eigenstate). The eigenvalues must be positive: $\nu_n^I \geq 0$ for all $n\{= 1, 2, \dots, 3(2I+1)\}$; 2) Define a matrix with the help of the eigenvalues ν^I and eigenstates χ^I :

$$\mathcal{H}_{nn'}^I = \sum_{KK'} \iint d\theta d\theta' \frac{\chi_n^{I*}(\theta; K)}{\sqrt{\nu_n^I}} H_{KK'}^I(\theta, \theta') \frac{\chi_{n'}^I(\theta'; K')}{\sqrt{\nu_{n'}^I}}. \quad (6)$$

The Hill-Wheeler equation then gets transformed into an ordinary eigenvalue equation in the basis of an orthonormal states. Then we solve the equation to obtain energy eigenvalues E^I and corresponding eigenfunctions.

Integration with respect to tilting angle θ in numerical calculations is achieved by an approximation of discretization: $\int d\theta \longrightarrow \sum \Delta\theta$. Normally the approximation becomes better as $\Delta\theta$ becomes smaller. One should note, however, that too fine discretization may lead to a problem of over-completeness in the GCM ansatz (Eq.2). We take $\Delta\theta = 6^\circ$. We then choose the maximum tilting angle $\theta_0=6^\circ$. This choice allows us to have the minimum effort in numerical calculations. The number of the discrete points may not be sufficient for a comparison with experimental data, but the calculation can give us enough information as long as we focus only on understanding of the mechanism of backbending involving high- K and low- K bands. In practice, we have already investigated that each 3d-CHFB state: $|\varphi(\theta)\rangle$ with $\theta = 0, \pm 6$, has about 0, $\pm 5\hbar$ K -component, respectively [15]. The net dimension of the matrix Eq.6 is hence $3 \times (2I+1)$. We must truncate at some order of the norm eigenvalue ν_n^I and reduce the dimension of the matrix Eq.6, because sometimes we had vanishingly small negative values of ν^I .

The negative values may be caused by numerical errors, for instance, in calculations of overlap kernels and in volume integrations of three dimensional manifold of Euler angles. There are several factors that we need to examine.

First of all, we examine precision of integration in the AMP operator. In the volume integral of the Euler angles we take 65 mesh points for α and γ whereas 481 points for β . The number of mesh points seems enough for obtaining reasonable accuracy. Integration formulae for discretization are the trapezoidal approximation for α and γ and the five-point approximation for β . This seems also reasonable because the overlap kernel has a periodic symmetry for α and γ while not for β .

Second, we examine precision of the overlap kernel. We evaluate the overlap kernel with the well-known formulae [12,17], which enable us to calculate the overlap kernels with the matrix elements of the generalized Bogoliubov transformation in the HFB method, and the interpolation method. There are two factors that may produce numerical errors in the overlap kernel: 1) Precision of the Wigner's function, i.e. D-function; 2) Unitarity of the generalized Bogoliubov transformation. We have checked the precision for both of these factors

and confirmed that corresponding errors are negligible. In this way, we have found no serious problem in our computation.

Around the projected angular momentum value $I \sim 13\hbar$, which is the same as the constrained value, the maximum value of the negative norm eigenvalue is of order 10^{-4} . We, therefore, truncate the number of states n in Eq.6 at this order. We keep about five states for the matrix Eq.6. (cf. multiplicity is about 1.71 for odd- I and 1.46 for even- I [15].) With this reduced matrix, we calculate energy eigenvalues and corresponding eigenfunctions. Eventually, we are able to obtain reliable results.

Fig.1 shows the resultant energy spectrum E^I . We can see a $\Delta I=2$ -band and a $\Delta I=1$ -band. Before backbending, the yrast and yrare bands correspond to $\Delta I=2$ -band and $\Delta I=1$ -band, respectively. They cross each other sharply with 97 KeV energy gap at $I = 12\hbar$. This fact indicates that the inter-band interaction is quite weak. Then after band crossing the $\Delta I=1$ -band becomes yrast and the $\Delta I=2$ -band continues above the yrast band.

It is interesting to see weight function $f_K^I(\theta)$ for each I to study a structure of each band because the weight function has information on the wave function $|\Phi_M^I\rangle$. Fig.2 (a set of graphs) shows the weight functions for the yrast and yrare bands appearing in Fig.1.

Before band crossing ($I = 10\hbar$), the yrast band is of a low- K ($K \sim 0$) character while the yrare band is of a high- K ($K \sim \pm 5$). Although in band crossing ($I = 12\hbar$) characters of the yrast and yrare bands are exchanged, we can see mixture of the two relevant bands: two small peaks of $f_K^I(\pm\theta_0)$ in $|K| \simeq 5$ in the yrare and a double-well of $f_K^I(0)$ near $K = 0$ in the yrast. These behaviors imply the existence of inter-band interaction. After band crossing ($I = 14\hbar$), the yrast state seems to be exchanged completely in position but we can see a trace of the mixture: height of the two peaks of $f_K^I(\pm\theta_0)$ around $|K| \simeq 5$ is a little bit decreased after band crossing. On the other hand, the yrare state is apparently a mixed state. In this manner, it is confirmed that our approach can handle a quantum effect (band-mixing) in the band crossing region through dynamical coupling of the bands, i.e., “wobbling motion”.

In the yrast state at $I = 10\hbar$, a major component is $K = 0$. Most of the $K = 0$ components are brought by a 3D-CHFB state with $\theta=0$, i.e., $|\varphi(0)\rangle$. The yrast state has hence a genuine character of principal axis rotating state (PAR) while

the yrare state has a character of tilted axis rotating state (TAR)².

These states before the band crossing are written as

$$|\Phi_{\text{yrast}}^I\rangle \propto \sum_{K>0} \frac{g_K^{\text{PAR}}}{1 + \delta_{K0}} \left\{ |\varphi_K^I(0)\rangle + |\varphi_{-K}^I(0)\rangle \right\} - \sum_K g_K^{\text{TAR}} \left\{ |\varphi_K^I(+\theta_0)\rangle + |\varphi_{-K}^I(-\theta_0)\rangle \right\}, \quad (7)$$

$$|\Phi_{\text{yrare}}^{even-I}\rangle \propto \sum_{K>0} \frac{g_K^{\text{PAR}}}{1 + \delta_{K0}} \left\{ |\varphi_K^I(0)\rangle + |\varphi_{-K}^I(0)\rangle \right\} + \sum_K g_K^{\text{TAR}} \left\{ |\varphi_K^I(+\theta_0)\rangle + |\varphi_{-K}^I(-\theta_0)\rangle \right\}, \quad (8)$$

and

$$|\Phi_{\text{yrare}}^{odd-I}\rangle \propto \sum_{K>0} g_K^{\text{PAR}} \left\{ |\varphi_K^I(+\theta_0)\rangle - |\varphi_{-K}^I(-\theta_0)\rangle \right\} - \sum_K g_K^{\text{TAR}} \left\{ |\varphi_K^I(+\theta_0)\rangle - |\varphi_{-K}^I(-\theta_0)\rangle \right\}, \quad (9)$$

where

$$|\varphi_K^I(\theta)\rangle \equiv \hat{P}_{MK}^I |\varphi(\theta)\rangle, \quad (10)$$

$$g_K^{\text{PAR}} = f_K^I(0) = f_{-K}^I(0) \quad \text{and} \quad g_K^{\text{TAR}} = f_K^I(\theta_0) = f_{-K}^I(-\theta_0). \quad (11)$$

With a relation

$$\hat{R}_x(\pi) |\varphi_K^I(\theta)\rangle = (-)^I |\varphi_{-K}^I(\theta)\rangle, \quad (12)$$

we can prove that all these states Eq.7-9, are eigenstates of $\hat{R}_x(\pi) = \exp(-i\pi\hat{J}_x)$ with its eigenvalue (so-called “signature”) $r = +1$. The x -axis is taken along the principal axis of the intrinsic quadrupole moment that is perpendicular to the symmetry axis [15].

² “TAR” used in this letter is different from an energetically stable 3d-CHFB solution, which we called “TAR” in a previous paper[14]. “TAR” in this letter means just a 3d-CHFB solution with non-zero tilting angle.

In this manner, the $\Delta I=2$ -band, i.e., yrast band before crossing, can be identified as a PAR-band while $\Delta I=1$ -band, i.e., yrare band before crossing, can be a TAR-band. Both of the bands have the same signature ($r = +1$). It is interesting that the TAR-band is able to have the signature ($r = +1$) due to superposition of states in the name of “wobbling motion”.

One of the reasons for weak inter-band interaction is that the K -distributions are so different in the PAR- and TAR-band that overlap of states between these bands are small. The signature does not play any role in this crossing. This discussion gives a possible explanation of the weak interaction between the g- and t-band in odd-odd nuclei such as ^{181}Re [8], and implies that simple two-band crossing of the g-band and the t-band may not be able to cause the “splitting” of the high- K band observed in even-even nuclei in the $A \simeq 180$ region [10].

Recently, a similar splitting is observed also in $K^\pi = 10^+$ band in ^{184}Os [18]. In this case, the splitting seems to occur after three-bands crossing of the g-, t- and s-bands. These bands come close to one another around $I \sim 15\hbar$ and cause inter-band transitions among themselves. The splitting occurs for $I \geq 16\hbar$. Phenomenological analysis using three-bands mixing calculation shows that the bands after crossing are highly mixed states of unperturbed g-, t- and s-bands. In particular, it is stressed that the strong interaction between the t- and s-bands plays an important role in producing the splitting.

In our calculation, there is no band similar to the s-band near the band crossing region. (The second excited band is $\Delta I=1$ -band and about 2 MeV higher than the yrare band.) This is because we select the generating states, i.e., 3d-CHFB solutions, with large gap energy (Δ). To improve our calculation, we should take into account states not only with large- Δ but also with small- Δ .

In conclusion, based on the variation after projection (GCM after AMP with 3d-CHFB states), we obtain energy spectrum showing two-bands with crossing of a low- K and a high- K band. The low- K and high- K bands are assigned to be PAR and TAR, respectively, from an analysis of the weight function $f_K^I(\theta)$; at low-spin, the yrast band has a PAR character while the yrare has a TAR character. They exchange their characters in band crossing region ($I = 12\hbar$) through a “wobbling mechanism” that is a coupling mode between low- K and high- K intrinsic structures. The interaction between the two bands is weak because the K -distributions of the bands are quite different though the bands

have the same signature ($r = +1$). The splitting, as proposed in Ref.[18], does not occur in our calculation. Three-bands crossing may be necessary to produce the splitting. Because of complicated band-mixing among these three bands, a quantum mechanical approach should be used in studying the phenomenon.

Authors are thankful to Dr. N. Tajima and Prof. A. Ansari for their useful advice. The numerical calculations are carried out at the Vector Parallel Processor, Fujitsu VPP500/28 at RIKEN. This work is financially supported in part by the Grant-in-Aid for Scientific Research from the Ministry of Education, Science, Sports and Culture of Japan (09640338)

References

- [1] A.Johnson, H.Ryde and S.A.Hjorth, Nucl. Phys. **A179** (1972) 753 ; A.Johnson, H.Ryde and J.Sztarkier, Phys. Lett. **34B** (1971) 605
- [2] P.Thieberger, Phys. Lett. **45B** (1973) 417
- [3] B.C.Smith and A.B.Volkov, Phys. Lett. **47B** (1973) 193
- [4] B.R.Mottelson and J.G.Valatin, Phys. Rev. Lett. **5** (1960) 511
- [5] F.S. Stephens and R.S. Simon, Nucl. Phys. **A183** (1972) 257
- [6] B.Banerjee, H.J.Mang and P.Ring, Nucl. Phys. **A215** (1973) 366
- [7] C.S.Purry et al, Nucl Phys. **A632** (1998) 229
- [8] C.J.Pearson et al., Phys. Rev. Lett. **79** (1997) 605
- [9] T.Shizuma et al, Nucl. Phys. **A593** (1995) 247
- [10] P.M. Walker et al., Phys. Lett. **B309** (1993) 14
- [11] S.Frauendorf, Nucl. Phys. **A557** (1993) 259c
- [12] N.Onishi and S.Yoshida, Nucl. Phys. **80** (1966) 367
- [13] E.Wüst and A.Anvari, Phys. Lett. **161B** (1985) 223
- [14] T. Horibata and N. Onishi, Nucl. Phys. **A596** (1996) 251 ; T.Horibata and N.Onishi, Phys. Lett. **B325** (1994) 283
- [15] M.Oi, N.Onishi, N.Tajima and T.Horibata, Phys. Lett. **B418** (1998) 1
- [16] T. Horibata, M. Oi and N. Onishi, Phys. Lett. **B355** (1995) 433
- [17] P.Ring and P.Schuck, *Nuclear Many-body Problem* (Springer Verlalg, Berlin,1980)
- [18] T.Shizuma et al., Phys. Lett. B in press

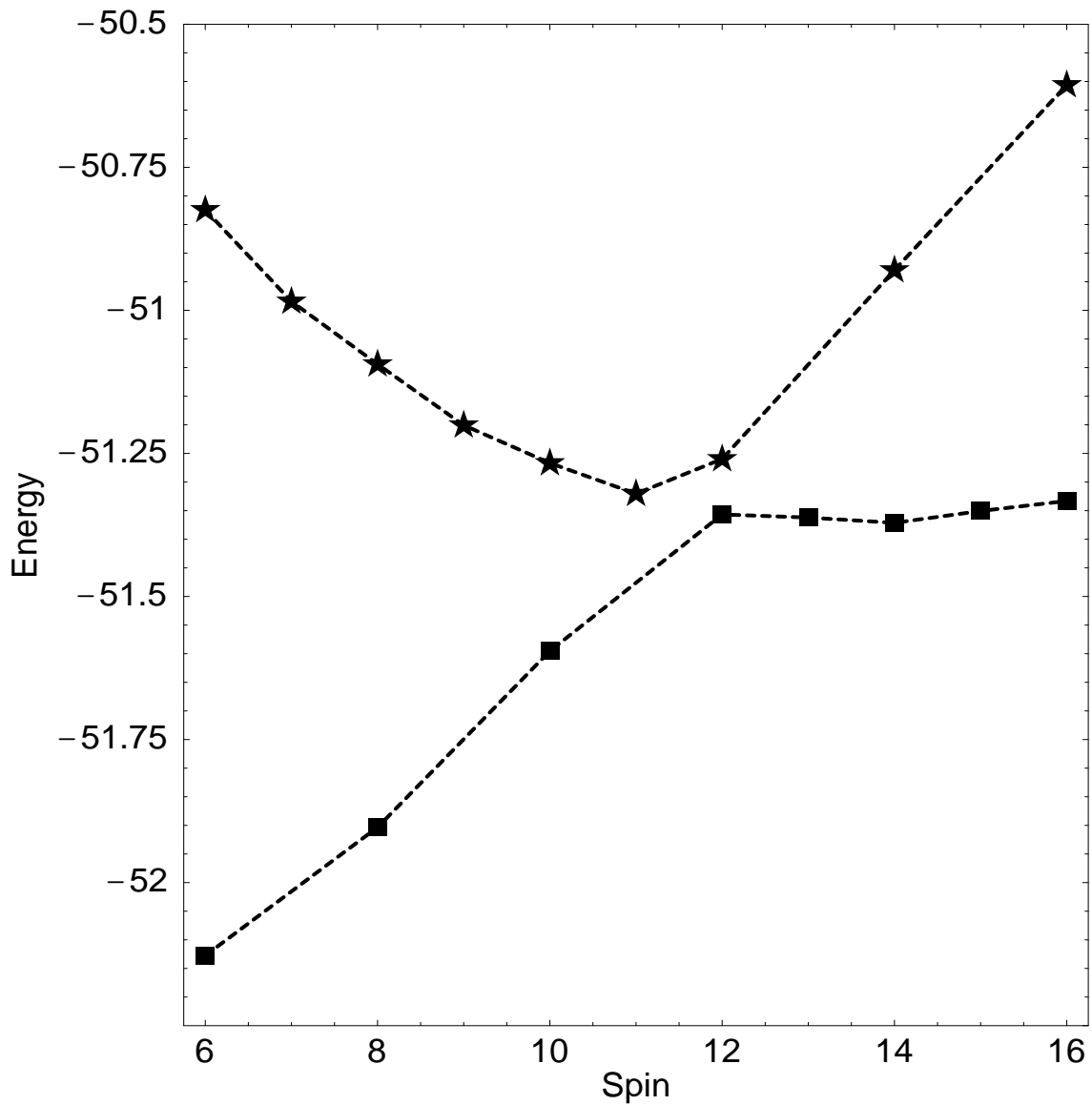


Fig. 1. Energy spectrum E^I (MeV), in which rotational energy, $0.01 \times I(I + 1)$, is subtracted from excited energy. A band crossing of $\Delta I=1$ -band with $\Delta I=2$ -band is seen at $I = 12\hbar$.

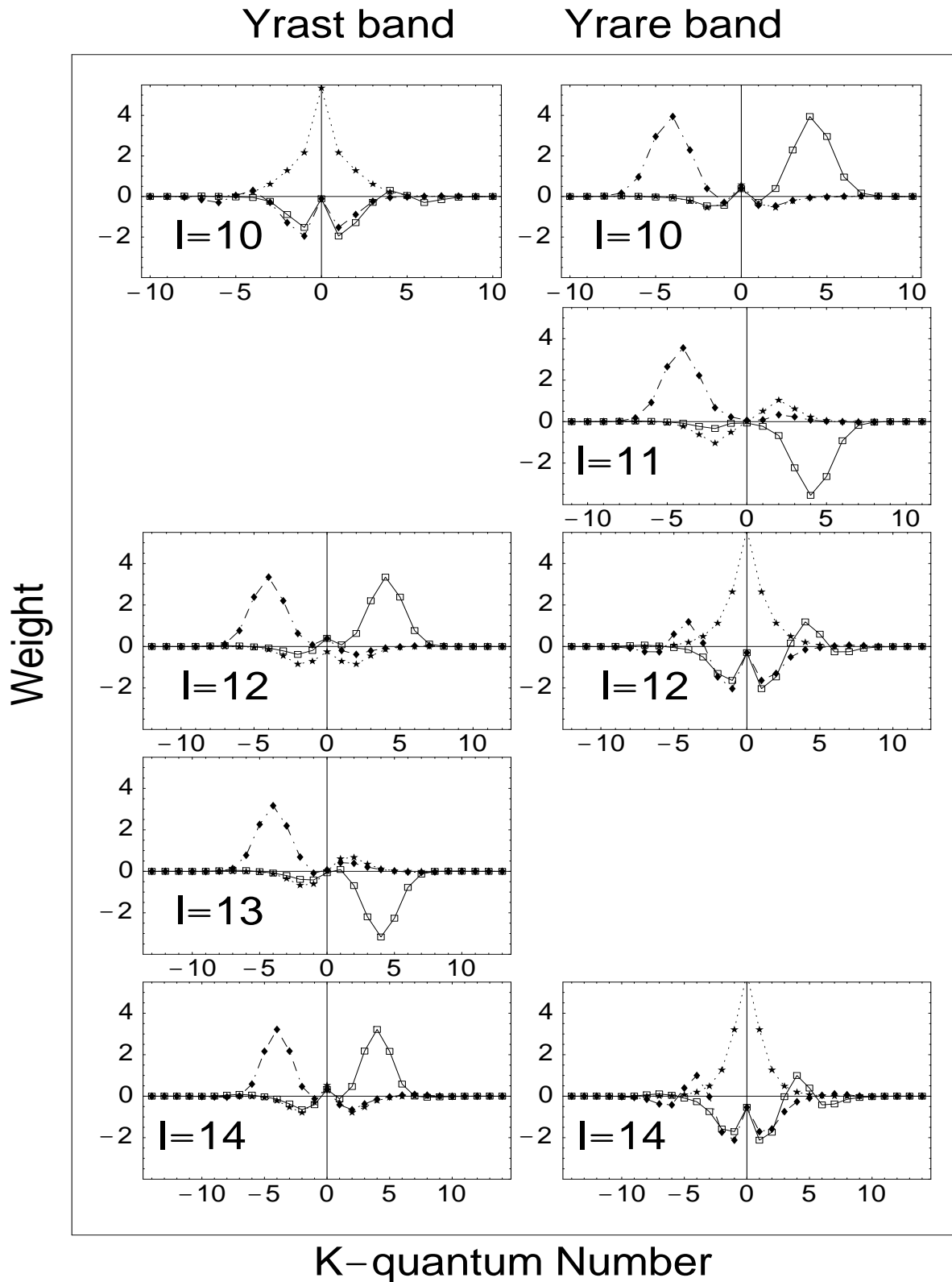


Fig. 2. Weight function $f_K^I(\theta)$ before ($I=10$ and 11), in ($I=12$), and after ($I=13$ and 14) backbending for the yrast (left column) and yrare (right column) bands. Curves for open squares, diamonds and stars in each graph show the weight function $f_K^I(+\theta_0)$, $f_K^I(-\theta_0)$ and $f_K^I(0)$, respectively.